Neuro-Oncology 14(4):496–505, 2012.
doi:10.1093/neuonc/nos069

Dynamic imaging response following radiation therapy predicts long-term outcomes for diffuse low-grade gliomas

Johan Pallud, Jean-François Llitjos, Frédéric Dhermain, Pascale Varlet, Edouard Dezamis, Bertrand Devaux, Raphaëlle Souillard-Scémama, Nader Sanai, Maria Koziak, Philippe Page, Michel Schlienger, Catherine Daumas-Duport, Jean-François Meder, Catherine Oppenheim, and François-Xavier Roux

Department of Neurosurgery, Sainte-Anne Hospital, Paris, France (J.P., J.-F.L., E.D., B.D., M.K., P.P., F.-X.R.); Université Paris Descartes, Paris, France (J.P., J.-F.L., P.V., E.D., B.D., R.S.-S., M.K., P.P., C.D.-D., J.-F.M., C.O., F.-X.R.); Department of Radiation Oncology and Physics, Institut Gustave Roussy, Villejuif Cedex, Paris, France (F.D.); Department of Neuropathology, Sainte-Anne Hospital, Paris, France (P.V., C.D.-D.); Department of Neuroradiology, Sainte-Anne Hospital, Paris, France (R.S.-S., J.-F.M., C.O.); Department of Oncology and Radiotherapy, Tenon Hospital, Paris, France (M.S.); Department of Neurosurgery, Barrow Neurological Institute, Phoenix, Arizona (N.S.); Réseau d'Etude des Gliomes, REG, Groland, France (J.P.)

Quantitative imaging assessment of radiation therapy (RT) for diffuse low-grade gliomas (DLGG) by measuring the velocity of diametric expansion (VDE) over time has never been studied. We assessed the VDE changes following RT and determined whether this parameter can serve as a prognostic factor. We reviewed a consecutive series of 33 adults with supratentorial DLGG treated with first-line RT with available imaging follow-up (median follow-up, 103 months). Before RT, all patients presented with a spontaneous tumor volume increase (positive VDE, mean 5.9 mm/year). After RT, all patients demonstrated a tumor volume decrease (negative VDE, mean, −16.7 mm/year) during a mean 49-month duration. In univariate analysis, initial tumor volume (>100 cm^3), lack of IDH1 expression, p53 expression, high proliferation index, and fast post-RT tumor volume decrease (VDE at −10 mm/year or faster, fast responders) were associated with a significantly shorter overall survival (OS). The median OS was significantly longer (120.8 months) for slow responders (post-RT VDE slower than −10.0 mm/year) than for fast responders (47.9 months). In multivariate analysis, fast responders, larger initial tumor volume, lack of IDH1 expression, and p53 expression were independent poor prognostic factors for OS. A high proliferation index was significantly more frequent in the fast responder subgroup than in the slow responder subgroup. We conclude that the pattern of post-RT VDE changes is an independent prognostic factor for DLGG and offers a quantitative parameter to predict long-term outcomes. We propose to monitor individually the post-RT VDE changes using MRI follow-up, with particular attention to fast responders.

Keywords: growth rates, low-grade glioma, prognosis, radiation therapy.

A better knowledge of the natural history of supratentorial hemispheric diffuse low-grade gliomas (DLGG) in adults has resulted in active therapeutic management of this tumor, and maximal safe resection while preserving eloquent brain areas is currently the first treatment option.[1–3] There is a consensus that the extent of resection is a prognostic factor for progression-free survival (PFS) and overall survival (OS).[1,4,5] However, for patients with unfavorable prognostic factors or for whom surgical resection is not feasible, an adjuvant treatment is indicated at any time, and radiation therapy (RT) is commonly administered.[1] Randomized studies have shown that RT prolongs PFS and helps control symptoms.[1,6–8]

Determining the efficacy of oncological treatments, particularly RT, poses several problems in patients with DLGG.[9] There are limited data describing the

Received September 20, 2011; accepted January 4, 2012.

Corresponding Author: Johan Pallud, MD, Service de Neurochirurgie, Hôpital Sainte-Anne, 1 rue Cabanis, 75674 Paris Cedex 14, France (johanpallud@hotmail.com).

patterns of response of DLGG to RT and no standard method for evaluating response. The measurement of the velocity of diametric expansion (VDE) of DLGG, estimated from the evolution of the mean tumor diameter (MTD) over time, can reliably quantify tumor growth on the basis of serial imaging.[10] All DLGG present a spontaneous tumor growth (a positive VDE, median VDE, at 4 mm/year), and the pretreatment VDE is a prognostic factor for OS.[11,12] In addition, VDE may be affected by oncological treatments: it remains unchanged after surgical resection[13] and decreases after procarbazine-CCNU-vincristine (PCV) and temozolomide chemotherapy.[14,15] Only rare observations of DLGG have reported a VDE change following RT.[16] However, the effect of RT on the VDE has not yet been studied in patients undergoing first-line RT.

The aim of the present study was to assess the VDE changes following RT and to determine whether this quantitative dynamic criterion can serve as a prognosis factor for long-term outcomes of supratentorial DLGG in adults. We hypothesized that the VDE patterns following RT predicted PFS and OS.

Patients and Methods

Selection Criteria

We retrospectively reviewed a series of consecutive adult patients with a DLGG diagnosed at the Sainte-Anne Hospital Center, Paris, France, from 1989–2010.

The following criteria were required: (1) patients older than 18 at histological diagnosis, (2) supratentorial hemispheric location (gliomatosis cerebri excluded), (3) absence of neurological deficit and of elevated intracranial pressure, (4) Karnofsky performance status (KPS) of 70 or more, (5) histological diagnosis of WHO grade II gliomas (gemistocytic astrocytoma excluded) obtained by a stereotactic biopsy procedure,[17,18] (6) absence of nodular-like or ring-like areas of contrast enhancement,[19] (7) available clinical and imaging follow-up to estimate VDE and Response Assessment in Neuro-Oncology (RANO) criteria for nonenhancing gliomas,[9] (8) RT as first-line oncological treatment without previous treatment except for stereotactic biopsy, and (9) RT initiation before any clinical or imaging evidence of malignant transformation.

Estimation of the Imaging Individual Tumor Growth Rates

The quantitative analysis of the imaging tumor growth (VDE) was performed on serial images before and after RT. Measurements were performed by 2 investigators (J.F.L., J.P.) while blinded to individual prognoses. The VDE was determined using a methodology previously described by Mandonnet et al.[10,11] consisting of manual measurements of the 3 largest tumor diameters in 3 orthogonal planes (axial, coronal, and sagittal) on successive MR examinations based on T2-weighted and Fluid Attenuated Inversion Recovery (FLAIR) sequences ($n = 354$), or on CT scan for a few examinations ($n = 25$) performed before the MRI era. The tumor volume was then calculated by an ellipsoid approximation, and the MTD was deduced from this volume. Finally, the VDE (the glioma growth curve) was plotted as a function of MTD over time. Thus, a positive VDE indicates a tumor volume increase, whereas a negative VDE indicates a tumor volume decrease. A mean of 11.6 ± 5.6 serial examinations (median 11, range 5–29) were available per patient.

Histological and Immunostaining Techniques

In our clinical practice, all DLGG were initially diagnosed according to the Sainte-Anne classification.[20–23] For study purposes, all tumors were reviewed according to the 2007 WHO classification of tumors of the central nervous system.[17,18] The biopsy samples were fixed by using glutar-zinc (6 cases) until 1992 and after 1992 by formalin-zinc (formalin 5%, zinc 3 g/L, sodium chloride 8 g/L) and then paraffin embedded. Proliferation rates were estimated for each patient with an index of MIB-1 immunostaining in the tumor area with the highest MIB-1–positive cell density. The percentage of MIB-1–positive cells was determined by counting cells in continuous microscopic fields at a magnification of ×400. A cutoff at 5% was established between a low and a high proliferation index. We analyzed p53 immunostaining using a monoclonal anti-p53 antibody (1/20, DO-1, Immunotech). Samples were considered to be negative for p53 accumulation when no or only rare nuclei were labeled. IDH1 immunostaining was performed with a Ventana automated system (BenchMark XT, Ventana Systems). A standard 1h pretreatment protocol included CC1 buffer and then an anti-IDH1-R132H antibody (1/200, clone DIA-H09, Dianova) for 32 min at room temperature. Antibody binding was visualized with the Ultraview DAB v3 kit (Ventana). IDH1 immunostatus was evaluated according to previous studies (identification of a single tumor cell in a tiny biopsy sample or in a mild infiltrative zone of a DLGG was considered to be positive).[24,25]

Statistical Analysis

Data for age (cutoff, 40 years), sex, KPS (cutoff, 70), tumor volumes at histological diagnosis and at RT initiation (cutoff, 100 cm^3), tumor midline crossing, p53 expression, IDH1 expression, proliferation index, spontaneous pre-RT VDE (cutoff, 8 mm/year), post-RT VDE (cutoff, −10 mm/year), post-RT MTD decrease (cutoff 20%), and post-RT tumor volume decrease (cutoff 50%) were obtained as baseline variables.[12,26]

Results are expressed as means ± standard deviation (SD; median, range). Groups were compared using χ^2 and Fisher's exact tests for categorical variables and Mann-Whitney rank-sum tests for continuous variables. Comparisons between related samples were performed

using Wilcoxon signed-rank tests. Kaplan-Meier analysis was used for unadjusted survival curves, using log-rank tests to assess significance. The primary endpoint was OS, measured from the date of histological diagnosis. The secondary endpoint was PFS, measured with 2 different methods from the date of histological diagnosis to (1) the date of imaging progression (the first evidence of tumor volume increase following RT; PFS according to VDE) and (2) the date of progression based on the recent clinical and radiological RANO criteria for nonenhancing gliomas (PFS according to RANO).[9] These intervals were censored at the date of last follow-up for survivors. Cox proportional hazards models were constructed, adjusting for predictors previously associated with mortality in univariate analysis. All statistical analyses were performed using JMP 7.2 software (SAS Institute). A significance level of $P < .05$ was used.

Results

Patient and Tumor Characteristics

Thirty-three patients (22 men, 11 women) met the eligibility criteria (Table 1). Mean patient age at histological diagnosis was 39.7 ± 10.3 years (median, 39.8; range. 23–66). Immuno-expression of p53, IDH1, and proliferation index could be evaluated in 27 (81.8%), in 27 (81.8%), and in 31 patients (93.9%), respectively, due to stereotactic biopsy material limitations and glutaraldehyde fixation techniques until 1992. p53 expression was present in 16 cases (59.3%, 16/27), IDH1 expression was present in 23 cases (85.2%, 23/27) and a high proliferation index was present in 13 cases (41.9%, 13/31). The spontaneous VDE was evaluated in only 19 patients (57.6%) because the initial MR examinations, performed in outside institutions before histological diagnosis, were unavailable in the remaining cases. All studied DLGG cases presented a spontaneous tumor volume increase, with a mean pre-RT spontaneous VDE of 5.9 ± 5.1 mm/year (median, 4.5; range, 0.6–16.9).

The external conformational RT was given using the same methodology (total dose, 50.4–54 Gy; 6-week period) at 2 outside institutions. The mean time interval between histological diagnosis and RT initiation was 10.4 ± 19.6 months (median, 2.0; range, 0–78).

Imaging Follow-up after Radiation Therapy

After RT, all patients had a tumor volume decrease (a negative VDE) during a mean of 49.0 ± 31.0 months (median, 42; range, 4.6–117.9) since histological diagnosis (Table 2). At the maximal imaging response, the mean tumor volume decrease was 60.3% ± 16.7% (median, 65.9; range, 11.7–87.0) and the mean MTD decrease was 28.5% ± 10.0% (median, 30.1; range, 4.6–49.3) compared with the tumor volume at RT initiation. The mean post-RT VDE was −16.7 ± 44.4 mm/year (median, −6; range, −1 to −256.2) during imaging response (Fig. 1). The post-RT VDE followed a gross linear decrease in 25 cases (75.8%), whereas the remaining cases followed a roughly exponential curve (Fig. 2). This second pattern resulted in a slight VDE overestimation when measurements were performed at 1 year post-RT compared with measurements performed throughout the duration of imaging response ($P = .043$) (Fig. 1). The post-RT VDE values varied considerably among patients, but their distribution resulted in 2 groups. Twenty-four patients (72.7%) presented a post-RT VDE slower than −10.0 mm/year (slow responders), and 9 (27.3%) presented a post-RT VDE of −10 mm/year or faster (fast responders). A high proliferation index was significantly more frequent in the fast responder subgroup (75%) than in the slow responder subgroup (30.5%) ($P = .04$). Similarly, the post-RT VDE was significantly faster in the high proliferation index subgroup than in the low proliferation index subgroup ($P = .015$) (Fig. 1). Sex, age at diagnosis, KPS, initial tumor volume and MTD, tumor midline crossing, pre-RT VDE, p53 expression, IDH expression, time interval between histological diagnosis and RT initiation, and time interval between initial oncological treatment and further treatment (data not shown) did not significantly differ between fast responder and slow responder subgroups. In the 19 patients with an available pre-RT VDE, the post-RT VDE did not significantly differ between low pre-RT VDE (under 8 mm/year) and high pre-RT VDE (8 mm/year or more) subgroups.

Imaging Progression Following Radiation Therapy

At various intervals following RT initiation (mean, 49 months; median, 42; range, 4.6–112.6), all tumors except 2 presented with imaging progression (a positive VDE) with an ongoing mean VDE at 7.8 ± 9.3 mm/year (median, 4.3; range, 1.3–43.5). Among these 31 patients, radiological progression was attributed to RT-induced changes in 2 patients (patients 6 and 13). In the remaining 29 patients, treatments at progression varied (chemotherapy alone, $n = 17$ [temozolomide, $n = 12$; PCV, $n = 3$; fotemustine, $n = 2$]; surgical resection alone, $n = 2$; second RT alone, $n = 1$; surgery plus second RT; $n = 2$; chemotherapy plus second chemotherapy, $n = 2$; surgery plus chemotherapy plus second chemotherapy, $n = 2$). One patient refused further oncological treatment (patient 21), and no additional treatment was deemed to be necessary in 2 patients (patients 30 and 32). Treatments at progression did not significantly differ between fast and slow responder subgroups.

The PFS according to VDE (mean, 49.0 ± 31.0; median, 42; range, 4.6–112.6) was significantly shorter than the PFS according to RANO (mean, 53.7 ± 41.9; median, 46.8; range, 3–188) ($P < .001$). In the 19 patients with an available pre-RT VDE, the low pre-RT VDE subgroup presented a slower VDE at imaging progression, a longer PFS according to VDE, and a longer PFS according to RANO than did the high pre-RT VDE subgroup, without the differences reaching statistical significance.

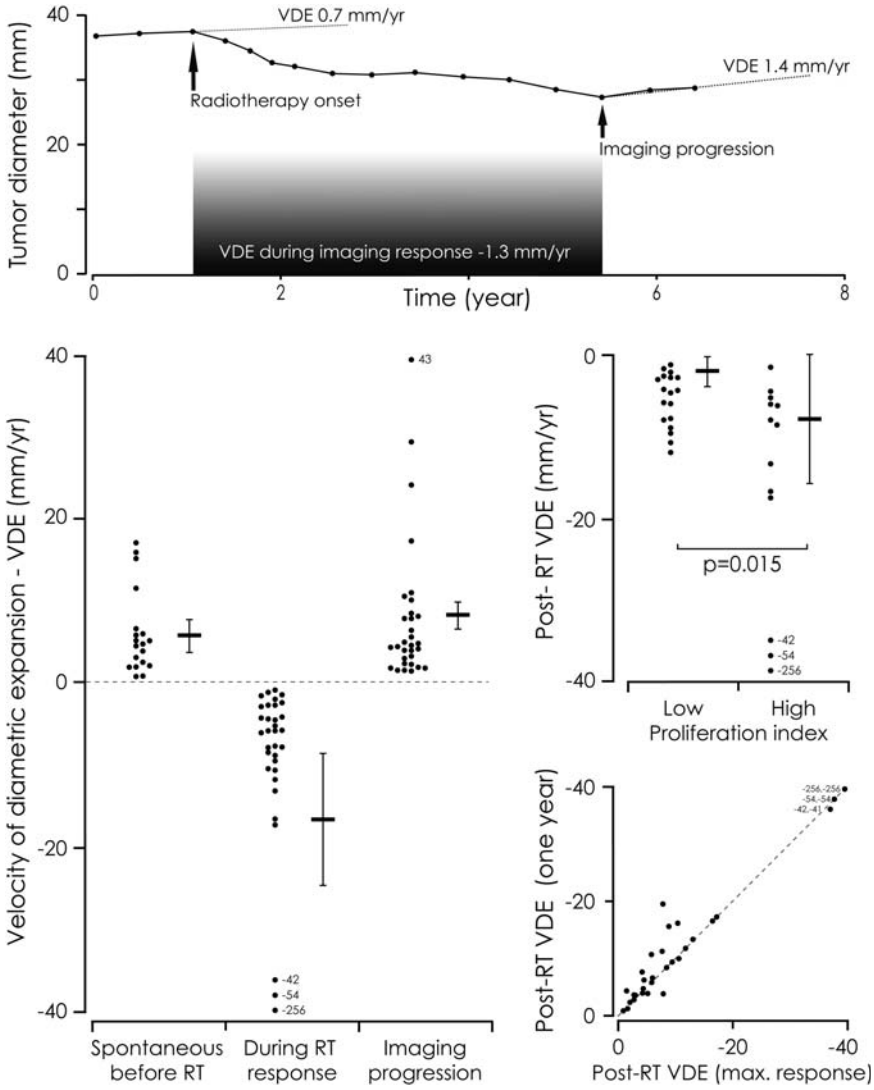

Fig. 1. *Top.* Example of the velocity of diametric expansion (VDE) of a diffuse low-grade glioma (DLGG) before and after radiation therapy (RT) (patient 3). Each point represents an MR examination. Before RT, the tumor grew spontaneously and continuously (positive VDE at 0.7 mm/year). After RT, the tumor volume decreased slowly (negative VDE at −1.3 mm/year). At imaging progression, the VDE increased at 1.4 mm/year. *Lower left.* Imaging VDE before and after RT. The results are expressed as means ± SEM. Before RT, the mean spontaneous VDE was 5.9 mm/year. Following RT, tumor volume decreased systematically in all patients, with a mean VDE of −16.7 mm/year. After various intervals following RT, all but 2 tumors presented an imaging progression with an ongoing mean VDE of 7.8 mm/year. *Middle right.* Distribution of the post-RT VDE according to proliferation index. The post-RT VDE were significantly faster in the high proliferation index subgroup than in the low proliferation index subgroup (Mann-Whitney test, $P = .015$). *Lower right.* Correlation of the post-RT VDE measured at 1 year post-RT initiation (vertical) and at the maximal imaging response (horizontal) in the 33 patients.

For PFS according to VDE, a high proliferation index ($P = .001$) and a post-RT VDE fast responder status ($P < .001$) were associated with a significant shorter PFS in univariate analysis. The median PFS according to VDE was 58.0 months in the slow responder subgroup and 24.1 months in the fast responder subgroup. Kaplan-Meier estimates for PFS according to VDE by post-RT VDE are shown in Fig. 3. In multivariate analysis, a post-RT VDE fast responder status (relative risk [RR], 5.4; $P = .003$), a large initial tumor volume (RR, 3.7; $P = .031$), and a high proliferation index (RR, 2.8; $P = .026$) were independent prognostic factors of shorter PFS according to VDE.

For PFS according to RANO, KPS ($P = .016$), a high pre-RT VDE ($P = .011$), a post-RT VDE fast responder status ($P = 0.042$), and a post-RT MTD decrease ($P = .016$) were associated with a significantly shorter PFS in univariate analysis. The median PFS according to RANO was 72.0 months in the slow responder subgroup and 24.3 months in the fast responder subgroup. In multivariate analysis, post-RT VDE fast responder status (RR, 2.4; $P = .05$), KPS (RR, 6.3; $P = .024$),

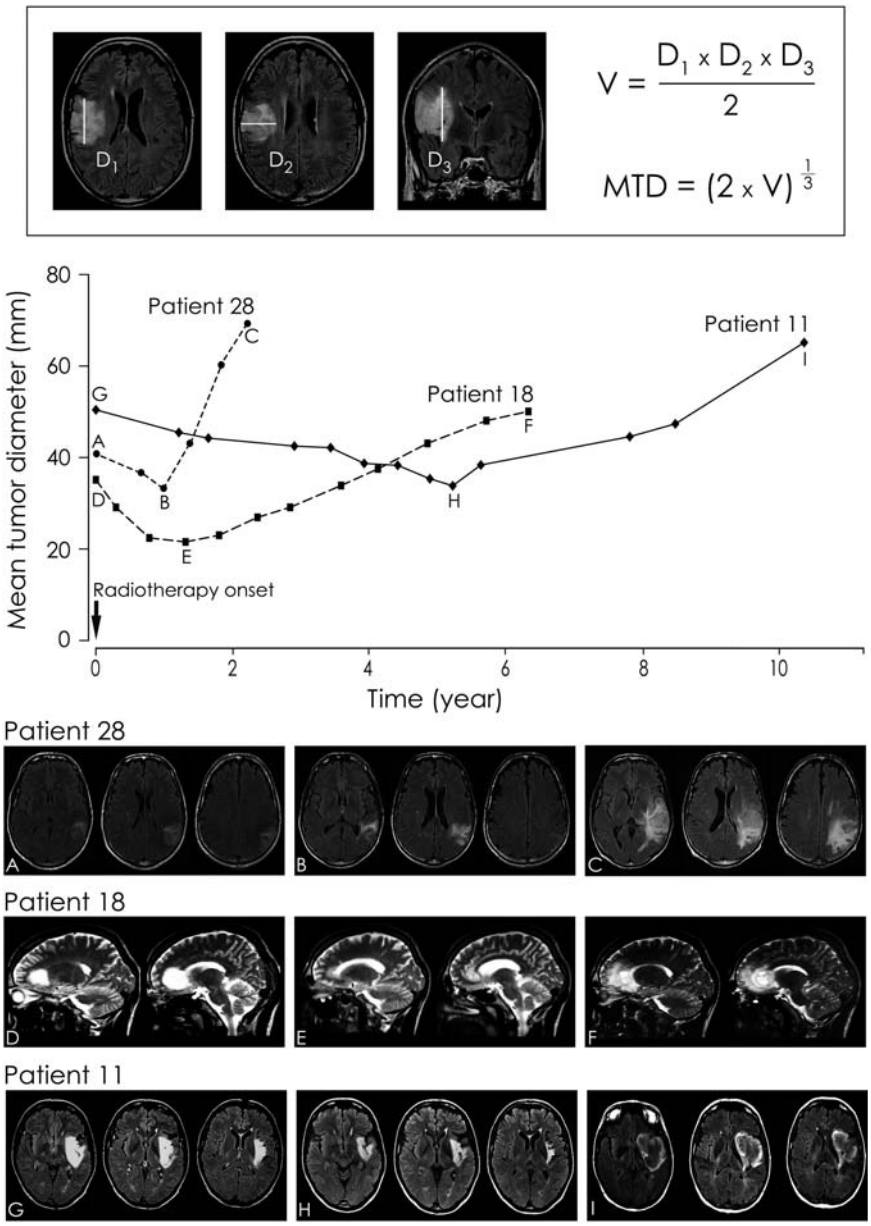

Fig. 2. *Top.* Measurement of the mean tumor diameter (MTD). The 3 largest tumor diameters in 3 orthogonal planes (axial, coronal, and sagittal) were manually measured. The tumor volume (V) was calculated by an ellipsoid approximation ($V = (D_1 \times D_2 \times D_3)/2$), and the MTD was deduced from the volume ($MTD = (2 \times V)^{1/3}$ *Bottom*. Examples of the evolution of the VDE following RT. The mean tumor diameter (mm) is plotted over time (years).

and post-RT MTD decrease (RR, 0.2; $P = .011$) were independent prognostic factors of shorter PFS according to RANO.

Survival Analyses

After a mean follow-up of 102.7 ± 69.8 months (median, 83.8; range, 24–262), 18 patients had died of oncological causes (54.5%) at a mean time of 68.4 ± 34.4 months from histological diagnosis. Thirteen of the remaining 15 patients presented clinical and/or imaging evidence of tumor progression. The median OS was 106.8 months (95% CI, 77.0–136.6) since histological diagnosis. Kaplan-Meier estimates for OS by post-RT VDE are shown in Fig. 3. Large initial tumor volume ($P = .025$), high proliferation index ($P = .05$), p53 expression ($P = .012$), lack of IDH1 expression ($P = .022$), high pre-RT VDE ($P = .002$), post-RT MTD decrease ($P = .007$), and post-RT VDE fast responder status ($P = .004$) were associated with a significantly shorter OS in univariate analysis. Importantly, the median OS was 120.8 months in the slow responder subgroup and 47.9 months in the fast responder subgroup. In multivariate analysis, large initial tumor volume (RR, 27.6; $P < .001$), lack of IDH1 expression (RR, 16.2; $P = .002$), post-RT VDE fast

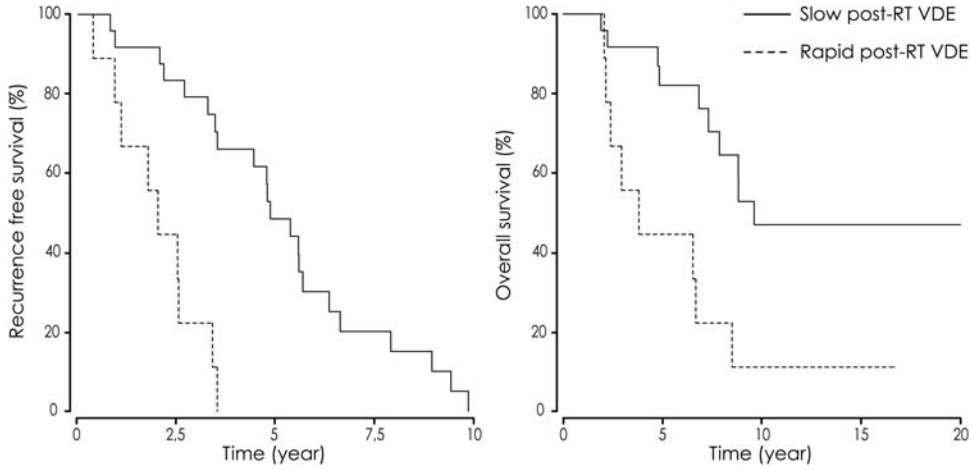

Fig. 3. Survival curves according to velocity of diametric expansion (VDE) following radiation therapy (RT). The median progression-free survival according to VDE was significantly longer for the slow responders (post-RT VDE slower than −10.0 mm/year) than for the fast responders (post-RT VDE of −10 mm/year or faster) ($P < .001$) (*left*). The median overall survival was significantly slower for the slow responders than for the fast responders ($P = .004$) (*right*).

responder status (RR, 5.1; $P = .019$), and p53 expression (RR, 4.9; $P = .028$) were independent prognostic factors of shorter OS.

Discussion

In the current study, we asked whether the imaging VDE assessment of DLGG obtained from the evolution of the MTD over time would help in monitoring and quantifying the effects of RT on an individual basis. Similar analyses were previously performed investigating surgical resection and chemotherapy,[13–15] with the following findings: (1) VDE of DLGG remained unchanged after surgical resection;[13] (2) almost all DLGG exhibited a tumor volume decrease after temozolomide initiation and showed different response patterns, depending on the 1p-19q codeletion status;[15] (3) all DLGG exhibited a tumor volume decrease after PCV chemotherapy initiation followed by a prolonged ongoing decrease after PCV discontinuation in 60% of cases.[14] Here, we provide the first quantitative evaluation of DLGG growth rates after RT based on serial MR examinations. We found that the VDE following RT represents a novel, quantitative, and independent prognostic factor for DLGG in adults treated with first-line RT. Specifically, we found that post-RT VDE slow responder status (slower than −10.0 mm/year) predicted a better outcome than post-RT VDE fast responder status (of −10 mm/year or faster) and was associated with better OS, better PFS according to VDE, and better PFS according to RANO.

The studied population although limited by the fact that spontaneous pre-RT VDE were available in only 19 cases (58%), presents homogeneous tumor findings (adults harboring a supratentorial tumor, IDH1 expression in more than 80% of cases, exclusion of most known risk factors, and all but 1 patient were considered "low-risk" according to the prognostic scoring system proposed by Pignatti et al.[26]). In addition, the patients had homogeneous oncological treatments (histological diagnosis by stereotactic biopsy only, RT protocols according to the current standard of care,[1] RT as first-line therapy before any sign of malignant transformation, and similar oncological treatments at progression). The observed long OS allowed survival analyses and searches for predictors. In our current practice, the first treatment option for DLGG is maximal safe surgical resection with functional monitoring associated with a close follow-up. Such patients are not referred to first-line RT. Thus, this homogeneous series does not strictly match the current indications of first-line RT for DLGG but reduces bias in the definition of prognostic parameters.

Here, we quantified for the first time the evolution of the MTD over time and the VDE changes before and after RT for DLGG. Determining the efficacy of therapies on the basis of serial imaging particularly RT, is challenging. Almost all patients experienced RT-induced white matter changes, rendering difficult the determination of reproducible imaging response parameters and their correlation with outcomes.[9,27] In a retrospective study of 21 adults receiving RT for DLGG, Bauman et al. did not detect a significant association between quantitative imaging response (linear, area, and volume measurements), symptoms, and PFS.[28] In a retrospective study of 19 children receiving RT for LGG, Fisher et al. quantified the volumetric tumor changes on serial CT scans and demonstrated a mean tumor volume decrease of 31% along a mean 14.4-month duration but failed to show a significant association between imaging changes and survival.[29] Because the actual distinction between the tumor itself and RT-induced changes is difficult and can limit the assessment of tumor response, we restricted our quantitative analysis to the period of imaging response following RT, before the occurrence of imaging progression. This reduces the risks of measurement errors by RT-induced changes. However, while we captured the overall

Table 1. Clinical, imaging, and pathological findings at histological diagnosis in the 33 patients with diffuse low-grade glioma

Patient Number	Sex	Age (years)	KPS	Tumor location	Side	Tumor volume (cm^3)	MTD (mm)	Tumor midline crossing	IDH expression	p53 expression	Proliferation index	Spontaneous VDE (mm/year)
1	F	36	90	Temporo-insular	L	56.6	48.4	No	–	–	–	–
2	M	43	90	Frontal	R	60.6	49.5	No	No	No	High	2.3
3	M	35	100	Frontal	R	19.2	33.7	No	–	–	Low	0.7
4	M	32	70	Fronto-parietal	L	121.2	62.3	No	Yes	Yes	High	15.7
5	F	53	80	Frontal	R	52.6	47.2	No	Yes	No	High	5.8
6	F	54	70	Cingular	L	17.8	32.9	No	–	No	Low	1.8
7	M	66	90	Frontal	R	6.5	23.6	No	No	Yes	High	4.5
8	M	30	80	Frontal	R	35.6	41.5	No	Yes	Yes	Low	1.9
9	M	39	90	Fronto-temporo-insular	R	117.7	61.8	Yes	Yes	Yes	Low	–
10	M	29	90	Frontal	R	25.5	37.1	No	Yes	Yes	Low	3.7
11	F	41	90	Temporo-insular	L	56.1	48.2	No	Yes	No	Low	5.0
12	M	40	90	Temporal	L	15.4	31.4	No	Yes	–	High	–
13	M	32	90	Parietal	R	66.3	51.0	No	–	–	Low	1.8
14	M	40	100	Temporo-insular	R	50.7	46.6	No	No	Yes	High	–
15	M	26	90	Parieto-temporo-insular	R	69.7	51.8	No	Yes	Yes	High	–
16	M	42	90	Frontal	L	7.1	24.2	No	Yes	Yes	Low	5.0
17	F	32	90	Fronto-temporo- insular	L	273.6	81.8	No	–	Yes	Low	–
18	M	23	70	Fronto-cingulo-callosal	R	10.0	27.1	Yes	Yes	Yes	–	11.3
19	M	39	90	Fronto-temporo-insular	R	55.5	48.1	No	Yes	Yes	Low	–
20	M	43	90	Parietal	R	27.1	37.8	No	Yes	Yes	Low	5.7
21	M	50	90	Temporo-insular	L	80.5	54.4	No	–	–	High	6.4
22	M	25	100	Frontal	R	48.0	45.8	No	Yes	No	Low	–
23	M	36	90	Fronto-temporo-insular	L	110.2	60.4	No	Yes	Yes	Low	2.9
24	F	31	100	Fronto-parietal	R	62.4	50.0	No	Yes	Yes	Low	4.3
25	F	44	80	Temporal	L	43.1	44.2	No	Yes	No	High	–
26	F	42	100	Frontal	R	27.4	38.0	Yes	Yes	Yes	Low	15.0
27	F	32	100	Fronto-insular	R	85.3	66.6	No	Yes	–	High	–
28	M	64	80	Parietal	L	32.5	40.2	No	No	–	High	16.90
29	M	50	90	Fronto-insular	R	81.7	54.7	No	Yes	No	Low	–
30	M	30	90	Parietal	L	23.4	36.1	No	Yes	–	High	0.6
31	F	40	90	Temporo-occipital	L	34.6	41.1	No	Yes	No	Low	–
32	M	48	100	Temporo-parieto-cingular	L	147.9	66.6	Yes	Yes	No	High	–
33	F	41	100	Temporo-parietal	R	112.3	60.8	No	Yes	Yes	Low	–

Abbreviations: KPS, Karnofsky performance status; MTD, mean tumor diameter; IDH, isocitrate dehydrogenase; VDE, velocity of diametric expansion.

Table 2. Imaging findings at radiation therapy initiation and during imaging follow-up in the 33 patients with diffuse low-grade glioma

Patient Number	At RT onset			Tumor volume decrease following RT					Tumor progression following RT			Survival	
	Time interval since histological diagnosis (months)	Tumor volume (cm^3)	MTD (mm)	Imaging RFS (months)	Tumor volume at the maximal imaging response		MTD at the maximal imaging response		VDE (mm/year)	Parameter based progression	Clinical RFS (months)	VDE (mm/year)	Follow-up (months)	Death
					(cm^3)	(%)	(mm)	(%)						
1	3	56.6	48.4	66.5	39.7	29.8	43.0	11.1	−1.0	Clinical	58	2.1	111	Yes
2	49	101.9	58.9	79.1	26.2	74.3	37.4	36.4	−7.9	Clinical	42	7.9	111	Yes
3	2	19.2	33.8	112.6	5.3	72.5	21.9	35.0	−1.3	MRI	188	1.4	260	–
4	7	199.5	73.6	13.0	34.9	82.5	41.2	44.1	−256.2	Clinical	3	24.3	26	Yes
5	2	56.6	47.2	42.0	8.4	85.2	25.0	47.1	−42.2	MRI	145	1.7	210	–
6	1	20.3	34.4	64.1	2.6	87.0	17.4	49.3	−2.9	Clinical	52	1.9	227	–
7	1	6.5	23.6	4.6	2.2	66.0	16.4	30.2	−54.1	Clinical	7	17.3	30	Yes
8	41	59.4	49.2	57.0	33.1	44.3	40.5	17.7	−9.6	MRI	17	4.2	86	Yes
9	2	138.6	65.2	9.7	122.4	11.7	62.2	4.6	−6.0	MRI	15	10.9	24	Yes
10	50	65.8	50.9	106.9	32.8	50.2	40.3	20.7	−2.2	MRI	58	3.7	209	–
11	2	46.5	50.5	67.9	19.1	58.9	33.7	25.6	−2.9	Clinical	92	5.6	129	–
12	1	15.4	31.4	24.7	7.1	53.8	24.3	22.4	−6.0	MRI	43	4.7	60	Yes
13	78	129.8	63.8	117.9	47.0	63.8	45.5	28.7	−7.8	Clinical	47	4.2	166	–
14	1	50.7	46.6	11.1	27.0	46.7	37.8	18.9	−13.2	Clinical	7	3.0	27	Yes
15	1	73.3	52.8	21.1	16.9	76.9	32.3	38.8	−17.3	Clinical	25	8.0	48	Yes
16	17	14.1	30.3	30.3	4.4	68.6	20.7	31.8	−10.7	MRI	39	2.8	107	Yes
17	1	273.6	81.8	41.4	86.5	68.4	55.7	31.9	−8.9	Clinical	71	4.9	99	Yes
18	7	21.4	35.0	24.0	4.9	76.9	21.5	38.7	−10.5	Clinical	5	6.2	84	Yes
19	3	69.7	51.8	40.6	41.3	40.7	43.6	16.0	−11.9	MRI	40	7.8	82	Yes
20	0	30.2	39.2	42.1	9.1	69.9	26.3	33.0	−4.7	MRI	124	1.4	262	–
21	0	80.5	55.5	24.1	26.8	66.6	37.7	32.1	−16.5	MRI	24	10.5	37	Yes
22	1	48.0	45.8	75.8	13.4	72.0	30.0	34.6	−8.0	MRI	76	3.8	121	Yes
23	1	161.5	68.6	58.0	51.6	68.1	46.9	31.6	−4.3	Clinical	46	43.5	61	Yes
24	52	158.2	68.1	94.4	79.8	49.5	52.1	23.5	−5.9	Clinical	56	4.3	186	–
25	1	43.1	44.2	57.1	10.8	75.0	27.8	37.0	−8.5	MRI	83	10.1	153	–
26	1	30.9	39.5	66.7	10.5	65.9	27.6	30.1	−2.7	MRI	80	4.3	92	Yes
27	3	85.3	66.6	32.1	51.4	39.7	46.8	29.7	−4.5	MRI	47	8.3	74	–
28	1	32.5	40.2	11.1	17.8	45.2	32.9	18.2	−6.2	MRI	21	29.5	28	Yes
29	1	81.7	54.7	39.2	27.6	66.2	38.1	30.3	−4.4	Clinical	51	1.3	57	–
30	3	23.4	36.1	53.0	8.7	62.8	25.9	28.3	−1.6	Progression no detected		1.5	67	–
31	6	34.6	41.1	–	20.2	41.6	34.3	16.5	−1.8	No progression		–	68	–
32	2	147.9	66.6	25.9	68.1	54.0	51.4	22.8	−5.3	MRI	51	2.1	57	–
33	2	112.3	60.8	–	51.0	54.6	46.7	23.2	−3.1	No progression		–	34	–

Abbreviations: KPS, Karnofsky performance status; MTD, mean tumor diameter; RT, radiation therapy; RFS, recurrence-free survival; VDE, velocity of diametric expansion.

imaging response following RT, we failed in assessing the exact component of imaging progression (tumor recurrence and/or RT-induced changes). Our current results will need to be reproduced in larger series from different institutions.

We have shown that VDE monitoring is possible following RT in clinical practice and may allow earlier prediction of poor outcomes. Indeed, VDE measured during the first year post-RT are grossly similar to VDE measured during the whole duration of imaging response. Of note, we used the 3-diameter technique for MTD measurements, because only printed MR images were available for older examinations. The limitations of this technique have been addressed,[10] and the gold standard remains the tumor 3-dimensional segmentation technique.

The mechanisms underlying the prolonged post-RT tumor volume decrease, rather than stabilization, remain to be determined for DLGG. This observation matches the tumor volume decrease observed during and after chemotherapy.[14,15] One may hypothesize that DLGG consists of different tumor cell components: proliferating and migrating cells, which would undergo apoptosis after a determined period, and nonproliferating nonmigrating (quiescent) cells. Without oncological treatment, the proliferation and the migration rates would be higher than the apoptosis rate, leading to spontaneous tumor growth (positive pre-RT VDE). Radiation therapy may inhibit proliferating and migrating cells, leading to a tumor decrease (negative post-RT VDE), and may damage quiescent cells, explaining the prolonged post-RT tumor volume decrease. This hypothesis may explain the present intriguing results: the slower the post-RT VDE change, the longer the PFS according to VDE and the better the clinical outcomes, including OS. Indeed we observed a significant link between post-RT VDE, PFS according to VDE, OS, and proliferation rates.

In conclusion, we demonstrated here that the pattern of post-RT VDE changes is a strong independent prognostic factor for supratentorial DLGG in adults. Quantifying dynamic imaging response after RT offers a quantitative parameter to predict long-term outcomes for DLGG. As the post-RT VDE and the PFS according to VDE appear to be more sensitive and to be earlier predictors than the PFS according to RANO, we suggest incorporating these parameters in the process of developing updated criteria to improve the assessment of response following RT in DLGG.[9]

As a practical consequence, we propose monitoring the VDE changes following RT on an individual basis by regular MRI follow-up in order to estimate long-term outcomes and anticipate tumor progression. We recommend particular attention to fast responders, because these patients may define a subgroup of DLGG at higher risk of undergoing initial malignant transformation.

Acknowledgments

We thank Françine Chassoux, Baris Turak, Georges Abi-Lahoud, François Nataf, and Elisabeth Landre, for their help in the data collection and Hugues Duffau, Luc Taillandier, and Emmanuel Mandonnet of the Réseau D'études des Gliomes (REG, France) and François Ducray for their helpful comments in the preparation of the manuscript. Authors J.P. and J.F.L. contributed equally to this work. Johan Pallud: literature search, study design, data collection, data analysis, data interpretation, figures and tables, and writing; Jean-François Llitjos: literature search, data collection, data analysis, figures and tables, and writing; Frederic Dhermain: data collection, data interpretation, writing; Edouard Dezamis: data collection, and study design; Bertrand Devaux: data collection, and writing; Nader Sanai: writing; Maria Koziak: data collection, writing; Philippe Page: data collection; Raphaëlle Souillard-Scémama: data collection, figures, and writing; Pascale Varlet: data collection, data interpretation, and writing; Michel Schlienger: data collection; Catherine Daumas-Duport: data collection; Jean-François Meder: data collection, and writing; Catherine Oppenheim: data interpretation, figures, and writing; François-Xavier Roux: study design, and writing.

Conflict of interest statement. None declared.

References

1. Soffietti R, Baumert BG, Bello L, et al. Guidelines on management of low-grade gliomas: report of an EFNS-EANO Task Force. *Eur J Neurol*. 2010;17:1124–1133.
2. Duffau H. Lessons from brain mapping in surgery for low-grade glioma: insights into associations between tumour and brain plasticity. *Lancet Neurol*. 2005;4:476–486.
3. Wessels PH, Weber WE, Raven G, et al. Supratentorial grade II astrocytoma: biological features and clinical course. *Lancet Neurol*. 2003; 2:395–403.
4. Sanai N, Mirzadeh Z, Berger MS. Functional outcome after language mapping for glioma resection. *N Engl J Med*. 2008;358:18–27.
5. Sanai N, Berger MS. Glioma extent of resection and its impact on patient outcome. *Neurosurgery*. 2008;62:753–764.
6. van den Bent MJ, Afra D, de Witte O, et al. Long-term efficacy of early versus delayed radiotherapy for low-grade astrocytoma and oligodendroglioma in adults: the EORTC 22845 randomised trial. *Lancet*. 2005;366:985–990.
7. Shaw E, Arusell R, Scheithauer B, et al. Prospective randomized trial of low- versus high-dose radiation therapy in adults with supratentorial low-grade glioma: initial report of a North Central Cancer Treatment Group/Radiation Therapy Oncology Group/Eastern Cooperative Oncology Group study. *J Clin Oncol*. 2002;20:2267–2276.

8. Karim AB, Maat B, Hatlevoll R, et al. A randomized trial on dose-response in radiation therapy of low-grade cerebral glioma: European Organization for Research and Treatment of Cancer (EORTC) Study 22844. *Int J Radiat Oncol Biol Phys*. 1996;36: 549–556.
9. van den Bent M, Wefel J, Schiff D, et al. Response assessment in neuro-oncology (a report of the RANO group): assessment of outcome in trials of diffuse low-grade gliomas. *Lancet Oncol*. 2011; 12:583–593.
10. Mandonnet E, Pallud J, Clatz O, et al. Computational modeling of the WHO grade II glioma dynamics: principles and applications to management paradigm. *Neurosurg Rev*. 2008;31:263–269.
11. Mandonnet E, Delattre JY, Tanguy ML, et al. Continuous growth of mean tumor diameter in a subset of grade II gliomas. *Ann Neurol*. 2003;53:524–528.
12. Pallud J, Mandonnet E, Duffau H, et al. Prognostic value of initial magnetic resonance imaging growth rates for World Health Organization grade II gliomas. *Ann Neurol*. 2006;60:380–383.
13. Mandonnet E, Pallud J, Fontaine D, et al. Inter- and intrapatients comparison of WHO grade II glioma kinetics before and after surgical resection. *Neurosurg Rev*. 2010;33:91–96.
14. Peyre M, Cartalat-Carel S, Meyronet D, et al. Prolonged response without prolonged chemotherapy: a lesson from PCV chemotherapy in low-grade gliomas. *Neuro Oncol*. 2010;12: 1078–1082.
15. Ricard D, Kaloshi G, Amiel-Benouaich A, et al. Dynamic history of low-grade gliomas before and after temozolomide treatment. *Ann Neurol*. 2007;61:484–490.
16. Pallud J, Duffau H, Razak RA, et al. Influence of pregnancy in the behavior of diffuse gliomas: clinical cases of a French glioma study group. *J Neurol*. 2009;256:2014–2020.
17. Reifenberger G, Kros JM, Louis DN, et al. Oligodendroglioma. In: Louis, DN, Ohgaki, H, Wiestler, OD, et al., eds. WHO Classification of Tumours of the Central Nervous System. Lyon: International Agency for Research on Cancer (IARC); 2007:54–59.
18. von Deimling A, Burger PC, Nakazato Y, et al. Diffuse astrocytomas. In: Louis, DN, Ohgaki, H, Wiestler, OD, et al., eds. WHO Classification of Tumours of the Central Nervous System. Lyon: International Agency for Research on Cancer (IARC); 2007:25–29.
19. Pallud J, Capelle L, Taillandier L, et al. Prognostic significance of imaging contrast enhancement for WHO grade II gliomas. *Neuro Oncol*. 2009;11:176–182.
20. Daumas-Duport C, Beuvon F, Varlet P, et al. [Gliomas: WHO and Sainte-Anne Hospital classifications]. *Ann Pathol*. 2000;20:413–428.
21. Daumas-Duport C, Tucker ML, Kolles H, et al. Oligodendrogliomas. Part II: A new grading system based on morphological and imaging criteria. *J Neurooncol*. 1997;34:61–78.
22. Daumas-Duport C, Varlet P, Tucker ML, et al. Oligodendrogliomas. Part I: Patterns of growth, histological diagnosis, clinical and imaging correlations: a study of 153 cases. *J Neurooncol*. 1997;34:37–59.
23. Pallud J, Varlet P, Devaux B, et al. Diffuse low-grade oligodendrogliomas extend beyond MRI-defined abnormalities. *Neurology*. 2010; 74:1724–1731.
24. Capper D, Reuss D, Schittenhelm J, et al. Mutation-specific IDH1 antibody differentiates oligodendrogliomas and oligoastrocytomas from other brain tumors with oligodendroglioma-like morphology. *Acta Neuropathol*. 2011;121:241–252.
25. Capper D, Weissert S, Balss J, et al. Characterization of R132H mutation-specific IDH1 antibody binding in brain tumors. *Brain Pathol*. 2010;20:245–254.
26. Pignatti F, van den Bent M, Curran D, et al. Prognostic factors for survival in adult patients with cerebral low-grade glioma. *J Clin Oncol*. 2002;20:2076–2084.
27. Wen PY, Norden AD, Drappatz J, et al. Response assessment challenges in clinical trials of gliomas. *Curr Oncol Rep*. 2010;12:68–75.
28. Bauman G, Pahapill P, MacDonald D, et al. Low grade glioma: a measuring radiographic response to radiotherapy. *Can J Neurol Sci*. 1999;26:18–22.
29. Fisher BJ, Bauman GS, Leighton CE, et al. Low-grade gliomas in children: tumor volume response to radiation. *J Neurosurg*. 1998;88:969–974.